

Exact solutions of the quantum double square well potential

Enrique Peacock-López^{1,*}

¹*Department of Chemistry
Williams College*

Williamstown, MA 01267

(Dated: June 13, 2006)

For a symmetrical quantum double square well potential, we find analytical expressions satisfied by the quantized energies. Graphical or numerical solutions of the former relations allow us to calculate normalization constants and construct the first eight solutions of the Schrödinger equation. With these exact solutions, we analyze quantum tunneling across a potential barrier and compare our results with the experimental data for ammonia.

INTRODUCTION

Most chemistry textbooks [1]-[15] in their quantum mechanics sections discuss, to different levels of analysis, the one-dimensional particle in a box (PIB) as a relevant one-dimensional quantum system. A natural application of the PIB considers delocalized π electrons in hydrocarbons or other organic compounds. In contrast with physicists [16]-[22], who usually consider other relevant one-dimensional potential related to scattering, chemists rarely consider other simple but chemically relevant one-dimensional potentials. In some textbooks [5]-[15] we find a qualitative discussion of quantum tunneling and barrier penetration but rarely a quantitative analysis.

Some advanced texts [5]-[15] may include a qualitative discussion of barrier penetration in two minima or double well potentials, but again no quantitative analysis. In a chemical system, the two minima potential corresponds, usually, to two equilibrium positions or molecular conformations. In the case of ammonia its so-called periodic inversion is a well documented example of quantum tunneling.

The energy level splitting resulting from barrier penetration is an important quantum mechanical effect that occurs whether the double well potential is symmetric or not. The internal rotation in CH_3CH_3 from one staggered configuration to another through an eclipsed positions at the top of the barrier is a good example of a symmetric potential. In contrast, in the cases of the asymmetric H_2O_2 hindered rotor or beryllium dicyclopentadienyl we encounter asymmetric double well potentials. Ammonia (NH_3), cyanamide (NH_2CN), PH_3 , and AsH_3 are chemical examples of symmetrical double well potentials where atoms can tunnel through the barrier. In the case of ammonia the double minima represents the possible nitrogen positions with respect to plane defined by the three hydrogens.

In the case of ammonia and similar molecules the vibrational level splitting due to barrier penetration has been observed through infrared (IR) spectroscopy. The ammonia double well potential can be approximated using the Manning potential [23] where the the depth or dis-

sociation energy is estimated to be about 5 eV and the height of the central barrier to be 0.25 eV. The quantitative analysis of the Manning [23] or similar potential [24] is quite difficult and only numerically tractable. As an alternative, some authors [7, 15, 18, 19, 21] consider a one-dimensional discontinuous infinite depth double well potential to emphasize the symmetry of the wave function and quantum tunneling, but none consider a quantitative analysis or a finite depth well.

In this paper we consider a double well finite depth potential as an approximation of the ammonia potential. In the second section we consider the discontinuous potential and its more general analytical solutions, as well as the continuity and smoothness conditions impose on the solutions of the Schrödinger equation by the quantum mechanical postulates. In the third section, we consider the boundary conditions that yield the allowed quantized energies, and we calculate step by step the resultant transcendental equation for the case of infinite depth and energy greater than the barrier height. All of the algebraic manipulations are straight forward and accessible to chemistry juniors with the typical mathematical background. In section four and five we calculate numerically the allowed energies and construct the first eight normalized wave function. In section six we discuss quantum tunneling. Direct comparison between our results and experimental data from ammonia is considered in section seven. Finally we summarize and offer some suggestion of how to use this paper in the classroom.

GENERAL SOLUTION

By dividing into five spatial regions, we set general differential equations derived from the Schrödinger equation (SE) and construct general solutions. The Double Square Well Potential (DSWP) is a simplified model of potentials found in molecular chemical systems where possible different conformations are separated by an energy barrier. Although the DSWP is a discontinuous function of position, it gives an appropriate and tractable description of the continuous double minima potentials. The DSWP is defined by the following piecewise function:

$$V(x) = \begin{cases} V_D & (L + \frac{a}{2}) \leq x < \infty \\ 0 & \frac{a}{2} < x < (L + \frac{a}{2}) \\ V_o & -\frac{a}{2} \leq x \leq \frac{a}{2} \\ 0 & -(L + \frac{a}{2}) < x < -\frac{a}{2} \\ V_D & -\infty < x \leq -(L + \frac{a}{2}) \end{cases} \quad (1)$$

where V_D is the depth or dissociation energy and V_o the height of the central barrier separating two equivalent spatial regions. Also notice that the potential is an even function of position, i.e., $V(-x) = V(x)$. Due to this symmetry, the solutions of the SE are either odd or even functions of position.

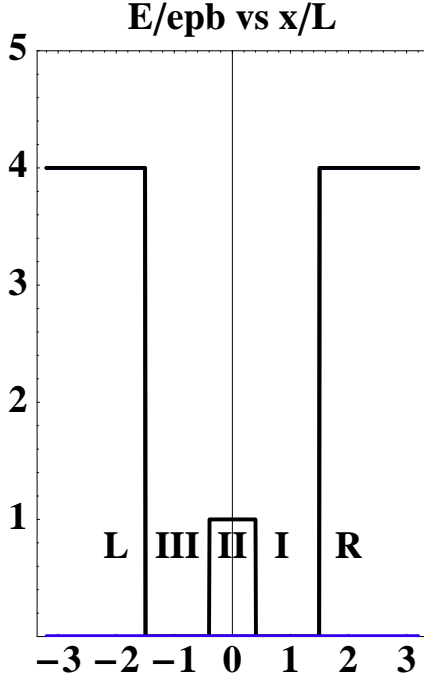


FIG. 1: The Double Well Square Potential diagram, where regions L, R, I, II, III are defined

Since the potential rises to the dissociation energy, V_D , for $|x| \geq L + a/2$ the SE,

$$-\frac{\hbar^2}{2m} \frac{d^2 \Psi_{RL}}{dx^2} + V_D \Psi_{RL} = E \Psi_{RL} \quad (2a)$$

for $E < V_D$ can be reduced to

$$\frac{d^2 \Psi_{RL}}{dx^2} = \kappa^2 \Psi_{RL} \quad (2b)$$

with

$$\kappa = \sqrt{\frac{8m\pi^2(V_D - E)}{h^2}} \quad (2c)$$

Now we consider the three internal spatial regions. First, we set the SE in each of the three spatial regions.

In region I, defined by $a/2 < x < L + a/2$, we have

$$-\frac{\hbar^2}{2m} \frac{d^2 \Psi_I}{dx^2} = E \Psi_I \quad (3a)$$

In region II, $|x| \leq a/2$, we need to include the constant potential V_o ,

$$-\frac{\hbar^2}{2m} \frac{d^2 \Psi_{II}}{dx^2} + V_o \Psi_{II} = E \Psi_{II} \quad (3b)$$

Finally, in region III, $-(L + a/2) < x < -a/2$,

$$-\frac{\hbar^2}{2m} \frac{d^2 \Psi_{III}}{dx^2} = E \Psi_{III} \quad (3c)$$

For regions I and III, we can reduce the SE to a simpler general equation

$$\frac{d^2 \Psi}{dx^2} = -\alpha^2 \Psi \quad (4a)$$

where we have defined

$$\alpha = \sqrt{\frac{8mE\pi^2}{h^2}} \quad (4b)$$

In region II we have two cases. In the first case the SE yields the following general equation:

$$\frac{d^2 \Psi_{II}^<}{dx^2} = \beta^{<2} \Psi_{II}^< \quad (5a)$$

where $E < V_o$, and we have defined

$$\beta^{<} \equiv \sqrt{\frac{8m\pi^2(V_o - E)}{h^2}} \quad (5b)$$

In the second case $E > V_o$ and we get

$$\frac{d^2 \Psi_{II}^>}{dx^2} = -\beta^{>2} \Psi_{II}^> \quad (6a)$$

with

$$\beta^{>} \equiv \sqrt{\frac{8m\pi^2(E - V_o)}{h^2}} \quad (6b)$$

Since α , $\beta^{>}$ and $\beta^{<}$ are positive real numbers, the solutions to eqs 4a, 6a are the simple and well known sine and cosine functions. In the case of eq 5a, the solutions are the hyperbolic sine and cosine, i.e., sinh and cosh.

The most general solution of the SE in each region is a linear combination of sine and cosine or sinh and cosh functions. Consequently we have six unknown coefficients that must be determined. The main problem in many of the one-dimensional quantum potentials is not the solution of the differential equations but finding coefficients that satisfy the required continuity and smoothness conditions at the regions' boundaries. In

other words, quantum mechanics requires that the piecewise wave function and its first derivative must be continuous. In our case, these conditions reduce to the following equations:

$$\Psi_{II}(a/2) = \Psi_I(a/2) \quad (7a)$$

$$\left. \frac{d \Psi_{II}}{d x} \right|_{x=a/2} = \left. \frac{d \Psi_I}{d x} \right|_{x=a/2} \quad (7b)$$

$$\Psi_{III}(-a/2) = \Psi_{II}(-a/2) \quad (7c)$$

$$\left. \frac{d \Psi_{III}}{d x} \right|_{x=-a/2} = \left. \frac{d \Psi_{II}}{d x} \right|_{x=-a/2} \quad (7d)$$

The continuity conditions at the edges of the potential region yield transcendental relations, whose solutions define the quantized energy levels for the DSWP

$$\Psi_I(L + a/2) = \Psi_R(L + a/2) \quad (8a)$$

$$\left. \frac{d \Psi_I}{d x} \right|_{x=L+a/2} = \left. \frac{d \Psi_R}{d x} \right|_{x=L+a/2} \quad (8b)$$

$$\Psi_{III}(-(L + a/2)) = \Psi_L(-(L + a/2)) \quad (8c)$$

$$\left. \frac{d \Psi_{III}}{d x} \right|_{x=-(L+a/2)} = \left. \frac{d \Psi_L}{d x} \right|_{x=-(L+a/2)} \quad (8d)$$

Finally, for $E < V_D$, we have the following limiting conditions

$$\lim_{x \rightarrow \infty} \Psi_R(x) = 0 \quad (9a)$$

$$\lim_{x \rightarrow -\infty} \Psi_L(x) = 0 \quad (9b)$$

These eight conditions determine the ten coefficients of the general solution of the SE for the DSWP. But we can considerably reduce the algebraic manipulations by recalling the potential symmetry and its implication to the solutions of the SE.

From eqs 2b, 9 we notice that the only possible solutions for $|x| \geq L + a/2$ are simple exponential functions

$$\Psi_R(x) = D_R \exp(-\kappa x) \quad (10a)$$

$$\Psi_L(x) = D_L \exp(\kappa x) \quad (10b)$$

Since the potential is an even function of position, the solutions of the SE are either even or odd functions of position,

$$\Psi(-x) = \pm \Psi(x). \quad (11)$$

As a consequence for $|x| \geq L + a/2$ we are required that D_R and D_L differ only by a sign, $D_L = \pm D_R$ depending on the symmetry of the wave function. In region II we are required to pick either an even or an odd function. In region III we pick the same coefficients as in region I. In other words, our general solution for $a/2 < x < L + a/2$ and $E > V_o$ reduces to

$$\Psi_I(x) = A \cos(\alpha x) + B \sin(\alpha x). \quad (12a)$$

For $-a/2 \leq x \leq a/2$ we have two choices, the symmetric or even function,

$$\Psi_{II}^S(x) = C^S \cos(\beta^> x), \quad (12b)$$

and the asymmetric or odd solution,

$$\Psi_{II}^A(x) = C^A \sin(\beta^> x). \quad (12c)$$

Finally for $-(L + a/2) < x < -a/2$, we have

$$\Psi_{III}^A = \pm \Psi_I(-x). \quad (12d)$$

where we pick the positive sign for the even solution and the negative sign for the odd solution. Notice that by considering the potential symmetry, we have reduced the number of coefficients and the chosen solution clearly shows the required symmetry.

In the case where $E < V_o$, we write the solution in region I as $a/2 < x < L + a/2$ and get

$$\Psi_I(x) = \bar{A} \sin(\alpha x) + \bar{B} \cos(\alpha x). \quad (13a)$$

where we have used over-barred coefficients to distinguish the $E < V_o$ case from the $E > V_o$ case.

For $-a/2 \leq x \leq a/2$ we substitute the sine and cosine functions in eqs 12b,12c by the corresponding hyperbolic function. In the even case we get

$$\Psi_{II}^S(x) = \bar{C}^S \cosh(\beta^< x), \quad (13b)$$

and in the odd case we get

$$\Psi_{II}^A(x) = \bar{C}^A \sinh(\beta^< x). \quad (13c)$$

Finally for $-(L + a/2) < x < -a/2$, we have

$$\Psi_{III}^A = \pm \Psi_I(-x). \quad (13d)$$

So far we have dealt with general results that have to be complemented by the boundary conditions to find particular solutions.

BOUNDARY CONDITIONS

In the previous section we found the most general solutions of the SE for the DSWP, but remember that quantum systems allow only a discrete set of energies,

$\{E_n\}$. These E_n are consistent with the the continuity and smoothness condition at the potential boundaries.

The most familiar boundary condition requires, as in the case of the particle in a box, that the wave function vanishes at the edges of the “box”, and, given the symmetry of the potential, we only have to consider one edge,

$$\Psi_I(L + a/2) = \Psi_R(L + a/2) \quad (14)$$

Using eq 10a, 12a we get

$$A \cos(\alpha(L + a/2)) + B \sin(\alpha(L + a/2)) = D_R \exp(-\kappa(L + a/2)) \quad (15a)$$

The slopes of the Ψ s yield a second condition

$$A \sin(\alpha(L + a/2)) - B \cos(\alpha(L + a/2)) = \frac{\kappa}{\alpha} D_R \exp(-\kappa(L + a/2)) \quad (15b)$$

Now we use eq 15a in eq 15b and rearrange the

$$A \left[1 + \frac{\alpha B}{\kappa A} \right] \cos(\alpha(L + a/2)) = -B \left[1 - \frac{\alpha A}{\kappa B} \right] \sin(\alpha(L + a/2)) \quad (16)$$

Equation 14 is satisfied in all possible cases, and we can recast it as

$$\tan(\alpha(L + a/2)) = -\frac{A}{B} F\left(A, B, \frac{\alpha}{\kappa}\right). \quad (17)$$

where we define

$$F\left(A, B, \frac{\alpha}{\kappa}\right) \equiv \frac{\left[1 + \frac{\alpha B}{\kappa A}\right]}{\left[1 - \frac{\alpha A}{\kappa B}\right]} \quad (18)$$

Equation 17 is a transcendental equation that we need to solve for the quantized energies, which are a consequence of the spatial constraint posed on the system. The exact solutions of eq 17 can only be obtained numerically, and we can do so in many different ways. In our approach we first rewrite eq 17 as

$$\alpha(L + a/2) = n\pi + \arctan\left(-\frac{A}{B} F\left(A, B, \frac{\alpha}{\kappa}\right)\right) \quad (19)$$

As we will show, once we fix the values of the mass, the length of the box, the thickness and the height of the barrier, and the depth of the potential, α , κ , A and B depend on the energy, E, and only a finite number of energies satisfy the relation expressed by equation eq 19.

Before proceeding with algebraic manipulations and finding expressions for the coefficients A and B, we rescale the spatial length and energy as follows:

$$\alpha x = \sqrt{\frac{8mL^2 V_o}{h^2}} \sqrt{\frac{E}{V_o}} \pi \frac{x}{L} \equiv \gamma c \pi X \quad (20a)$$

$$\kappa x \equiv \gamma \sqrt{D^2 - c^2} \pi X \quad (20b)$$

$$D \equiv \sqrt{\frac{V_D}{V_o}} \quad (20c)$$

$$\beta^< x = \gamma \sqrt{1 - c^2} \pi X \quad (20d)$$

$$\beta^> x = \gamma \sqrt{c^2 - 1} \pi X \quad (20e)$$

$$r \equiv \frac{a}{2L} \quad (20f)$$

In eq 20a, γ^2 represent the height of the barrier in units of epb defined as

$$epb \equiv \frac{h^2}{8mL^2}, \quad (21)$$

which is determined by the the mass of the particle and the length of the box. Also c^2 represents the ratio of the system's energy to the height of the barrier, and finally X is the distance in units of L.

Now we are ready to consider the even and odd solutions for $E > V_o$ and $E < V_o$ and to analyze the boundary conditions expressed by eqs 7. First we consider $E > V_o$ or $c > 1$, and we find that the even solution at $x = a/2$ satisfies the following continuity condition:

$$A^S \cos(\gamma c \pi r) + B^S \sin(\gamma c \pi r) = C^S \cos(\gamma \sqrt{c^2 - 1} \pi r) \quad (22a)$$

In the case of the smoothness condition we get

$$A^S \sin(\gamma c \pi r) - B^S \cos(\gamma c \pi r) = C^S \sqrt{1 - \frac{1}{c^2}} \sin(\gamma \sqrt{c^2 - 1} \pi r) \quad (22b)$$

We can solve for A if we first multiply eq 22a by $\cos(\gamma c \pi r)$ and eq 22b by $\sin(\gamma c \pi r)$. Second we add the resulting equations, and since $\sin^2 + \cos^2 = 1$ we find that A^S is given by the following expression:

$$A^S = C^S \left[\cos(\gamma c \pi r) \cos(\gamma \sqrt{c^2 - 1} \pi r) + \sqrt{1 - \frac{1}{c^2}} \sin(\gamma c \pi r) \sin(\gamma \sqrt{c^2 - 1} \pi r) \right] \quad (23a)$$

Now we can multiply Eq.(22a) by \sin and we subtract eq 22b multiplied by \cos . So we get

$$B^S = C^S \left[\sin(\gamma c \pi r) \cos(\gamma \sqrt{c^2 - 1} \pi r) - \sqrt{1 - \frac{1}{c^2}} \cos(\gamma c \pi r) \sin(\gamma \sqrt{c^2 - 1} \pi r) \right] \quad (23b)$$

Notice that both A and B are expressed as function of C^S that can be calculated numerically using the required

Now we are ready to consider the even and odd solutions for $E > V_o$ and $E < V_o$ and to analyze the boundary conditions expressed by eqs 7. First we consider $E > V_o$ or $c > 1$, and we find that the even solution at $x = a/2$ satisfies the following continuity condition:

$$\begin{aligned} A^S \cos(\gamma c \pi r) + B^S \sin(\gamma c \pi r) \\ = C^S \cos(\gamma \sqrt{c^2 - 1} \pi r) \end{aligned} \quad (22a)$$

In the case of the smoothness condition we get

$$\begin{aligned} A^S \sin(\gamma c \pi r) - B^S \cos(\gamma c \pi r) \\ = C^S \sqrt{1 - \frac{1}{c^2}} \sin(\gamma \sqrt{c^2 - 1} \pi r) \end{aligned} \quad (22b)$$

We can solve for A if we first multiply eq 22a by $\cos(\gamma c \pi r)$ and eq 22b by $\sin(\gamma c \pi r)$. Second we add the resulting equations, and since $\sin^2 + \cos^2 = 1$ we find that A^S is given by the following expression:

$$\begin{aligned} A^S = C^S \left[\cos(\gamma c \pi r) \cos(\gamma \sqrt{c^2 - 1} \pi r) + \right. \\ \left. \sqrt{1 - \frac{1}{c^2}} \sin(\gamma c \pi r) \sin(\gamma \sqrt{c^2 - 1} \pi r) \right] \end{aligned} \quad (23a)$$

Now we can multiply Eq.(22a) by \sin and we subtract eq 22b multiplied by \cos . So we get

$$\begin{aligned} B^S = C^S \left[\sin(\gamma c \pi r) \cos(\gamma \sqrt{c^2 - 1} \pi r) - \right. \\ \left. \sqrt{1 - \frac{1}{c^2}} \cos(\gamma c \pi r) \sin(\gamma \sqrt{c^2 - 1} \pi r) \right] \end{aligned} \quad (23b)$$

Notice that both A and B are expressed as function of C^s that can be calculated numerically using the required quantum mechanical normalization conditions on the solutions of the SE.

In the case of the asymmetric (odd) solution for $E > V_o$ we get that the continuity and smoothness conditions yield the following relations:

$$\begin{aligned} A^A \cos(\gamma c \pi r) + B^A \sin(\gamma c \pi r) \\ = C^A \sin(\gamma \sqrt{c^2 - 1} \pi r) \end{aligned} \quad (24a)$$

$$\begin{aligned} A^A \sin(\gamma c \pi r) - B^A \cos(\gamma c \pi r) \\ = - C^A \sqrt{1 - \frac{1}{c^2}} \cos(\gamma \sqrt{c^2 - 1} \pi r) \end{aligned} \quad (24b)$$

Now we multiply eq 24a by $\cos(\gamma c \pi r)$ and eq 24b by $\sin(\gamma c \pi r)$, and we add the resulting equations to get an expression for A^A

$$A^A = C^A \left[\cos(\gamma c \pi r) \sin \left(\gamma \sqrt{c^2 - 1} \pi r \right) - \sqrt{1 - \frac{1}{c^2}} \sin(\gamma c \pi r) \cos \left(\gamma \sqrt{c^2 - 1} \pi r \right) \right] \quad (25a)$$

Finally, we multiply eq 24a by \sin and we subtract eq 24b multiplied by \cos , and we get

$$B^A = C^A \left[\sin(\gamma c \pi r) \sin \left(\gamma \sqrt{c^2 - 1} \pi r \right) + \sqrt{1 - \frac{1}{c^2}} \cos(\gamma c \pi r) \cos \left(\gamma \sqrt{c^2 - 1} \pi r \right) \right] \quad (25b)$$

Now we can rewrite eq 19 as

$$\gamma c (1 + r) = n + \frac{1}{\pi} \arctan \left(-\frac{A}{B} F \left(A, B, \frac{\alpha}{\kappa} \right) \right) \quad (26a)$$

where

$$\frac{\alpha}{\kappa} = \frac{c}{\sqrt{D^2 - c^2}} \quad (26b)$$

Consequently we can substitute the corresponding expression for A and B from eqs 23a, 23b for the symmetric case and eqs 25a, 25b for the asymmetric case in eq. 26a. Notice that if we measure energy in units of epb , eq 21, and distance in units of L , and we fix the height, V_o , and the width, a , of the barrier, we then fix the values of γ and r . Therefore we are left with a transcendental equation for c , which is associated with the allowed energy eigenvalues, E .

IV. EXACT SOLUTION FOR $V_D \gg E > V_o$

The case $V_D \gg E > V_o$ implies that $D \gg c$ so $\alpha/\kappa \rightarrow 0$ and $F(A, B, \alpha/\kappa) \rightarrow 1$. Therefore eq 26a is simplified and independent of V_D . So far we have exact analytical relations satisfied by the system's allowed energies, but we can only solve the transcendental equation, eq 26a, numerically. For practical purpose, we solve eq 26a graphically by plotting first the right-hand side of eq 26a for different values of n , and second by plotting the left-hand side of eq 26a. The intersections give us the solutions of the transcendental equation and from these values we get the allowed energies.

In the present analysis, we consider the first two solutions for $r = 0.20$ and $V_o = 8 epb$. This last condition implies that $\gamma = \sqrt{8}$. In Figure 2 we depict the graphical method and

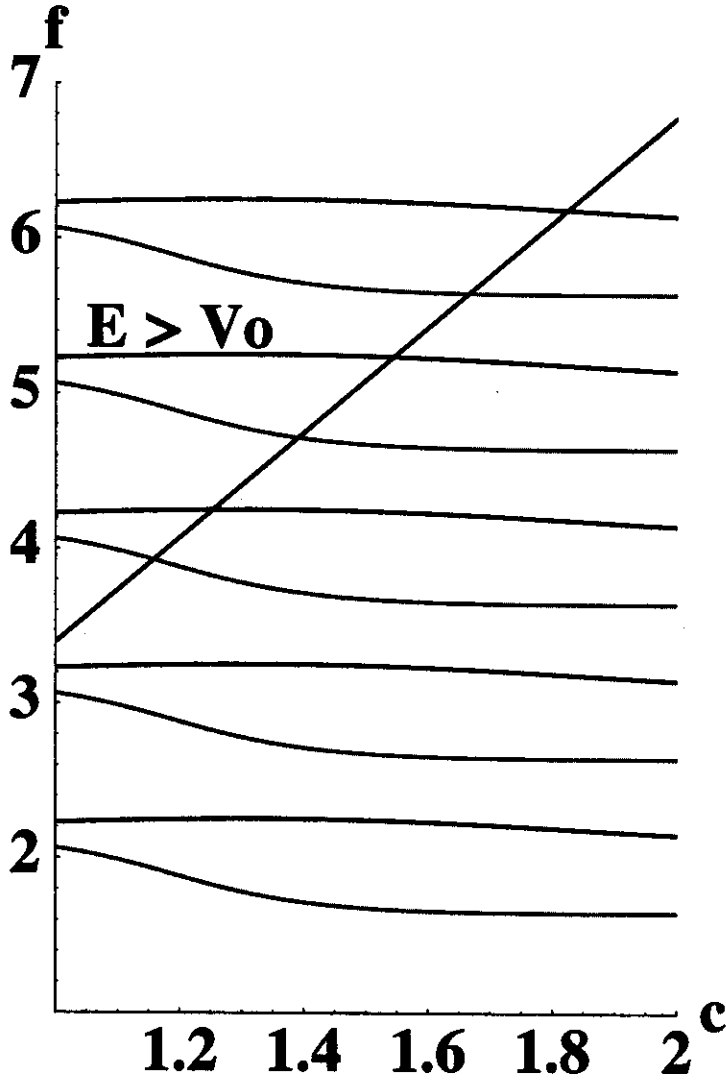


FIG. 2: Graphical solutions of eq 26a) for $\gamma = \sqrt{8}$ and $r=0.20$, and $c > 1$. For each value of n , the lower curve corresponds to the even case, and the the upper curve to the odd case.

notice that there are no solutions for $n \leq 3$ and $c = \sqrt{E/V_0} \geq 1$. For $n = 4$ we find $c_4^S = 1.16$ and $c_4^A = 1.255$, and these values yield the following energies:

$$E_7 = 1.35 V_0 \quad (27)$$

$$E_8 = 1.58 V_0 \quad (28)$$

which are the first two energy levels above the barrier.

Next we can use the numerical values of c_4^S and c_4^A , $\gamma = \sqrt{8}$, and $r = 0.20$ in eqs 12) and

construct the even wave function

$$\Phi_4^S(X) = \begin{cases} 0 & (1+r) \leq X < \infty \\ \Psi_I^{4S}(X) & r < X < (1+r) \\ \Psi_{II}^{4S}(X) & -r \leq X \leq r \\ \Psi_I^{4S}(-X) & -(1+r) < X < -r \\ 0 & -\infty < X \leq -(1+r) \end{cases} \quad (29)$$

where

$$\Psi_I^{4S}(X) = A_4^S \cos(\gamma c_4^S \pi X) + B_4^S \sin(\gamma c_4^S \pi X) \quad (30)$$

and

$$\Psi_{II}^{4S}(X) = C_4^S \cos\left(\gamma \sqrt{(c_4^S)^2 - 1} \pi X\right) \quad (31)$$

To get numerical values of Φ_4^S we need to use eqs 23a, 23b to get the expressions for A_4^S and B_4^S as functions of γ , r , $c_4^S = 1.16$, and C_4^S . Notice that Φ_4^S is defined, so far, up to an undetermined constant C_4^S that normalizes Φ_4^S . In other words, C_4^S is such that

$$\int_{-(1+r)}^{1+r} |\Phi_4^S(X)|^2 dX = |C_4^S|^2 (0.705) = 1 \quad (32)$$

Therefore $C_4^S = 1.191$ and now we have a normalized wave function, $\Phi_4^S(X)$.

To solve eq 26a for the asymmetric (odd) solution we need analytical expressions for A and B. In Appendix A we consider the odd solution $\Phi_4^A(X)$, and express in Eqs.(25a-25b) the required coefficients. In Figure 3 we depict these even and odd normalized solutions for $\gamma = \sqrt{8}$, $r = 0.20$.

V. EXACT SOLUTION FOR $V_D \gg V_o > E$

In this case, we consider all the solutions for $n \leq 3$, $c < 1$, $V_o = 8$ epb, and $r = 0.20$. We also use eq 45a-47b in Appendix B for the A and B coefficients needed to solve Eq.(26a). In Figure 4 we depict the graphical method and notice that there are six solutions. In practice, we blow-up the plot in Figure 4 to find the solutions up to the three significative figures that are enough for this analysis. In Table 1, we show the first six energy levels for the DSWP, and in Figure (5) we depict the first eight energy levels with respect to the barrier's height.

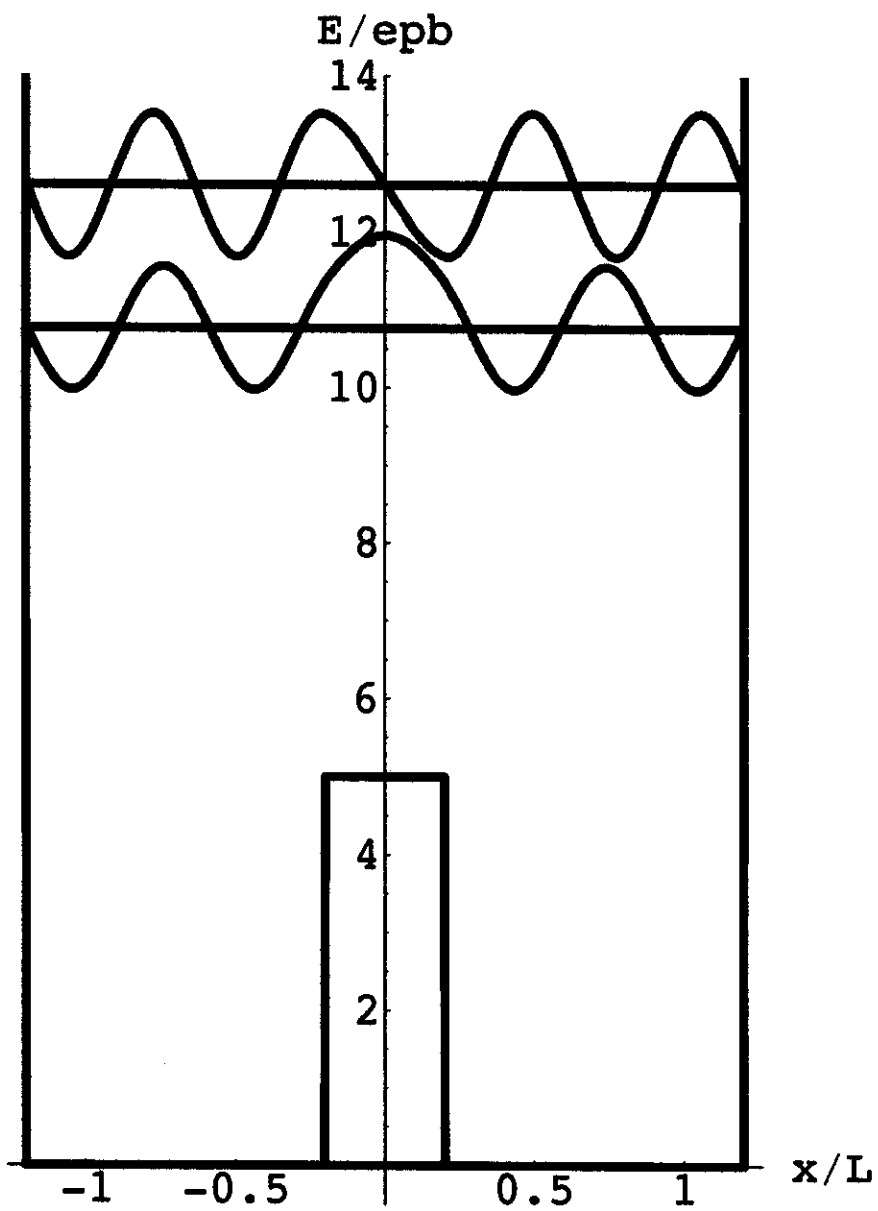


FIG. 3: First two solutions , (Φ_4^S, Φ_4^A) , for $E > V_0$.

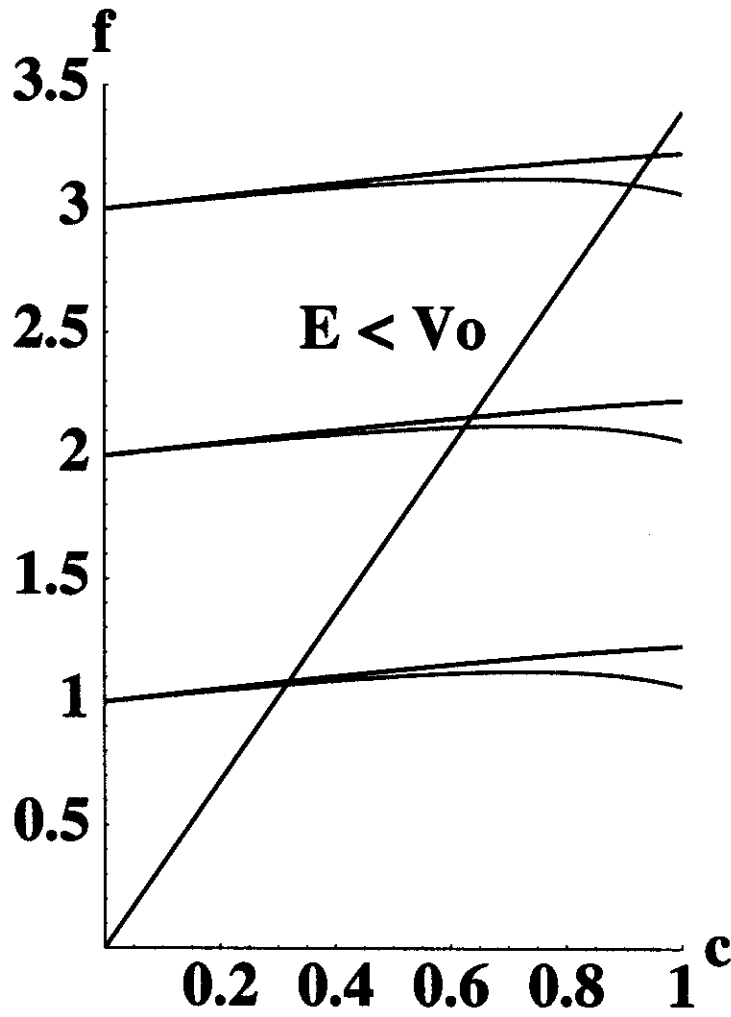


FIG. 4: Graphical solutions of Eq.(26a) for $\gamma = \sqrt{8}$, $c \leq 1$ and $r = 0.20$. For each value of n , the lower curve corresponds to the even case, and the the upper curve to the odd case.

TABLE 1	
$E < V_0$	
c_i	$E_i = c_i^2(V_0/epb)$
$c_1^S = 0.315$	$E_1 = 0.794$
$c_1^A = 0.319$	$E_2 = 0.814$
$c_2^S = 0.624$	$E_3 = 3.12$
$c_2^A = 0.636$	$E_4 = 3.24$
$c_3^S = 0.914$	$E_5 = 6.68$
$c_3^A = 0.949$	$E_6 = 7.20$

As in the case of the ammonia potential, we observe the progressive ting, $\Delta E_{21} < \Delta E_{34} < \Delta E_{65}$, between the energies associated with the adjacent symmetric and asymmetric solutions. Notice that we purposely consider a set of parameters such that only the first six energies are less than the barrier's height as in the case of ammonia. From our analytical results, we are able to observe that when the barrier height increases the number of energies less than the barrier's height also increases, but the energy difference between adjacent symmetric and asymmetric solutions decreases.

Next we can use the numerical values in Table 1, $\gamma = \sqrt{8}$, and $r = 0.20$ in eq 13 to construct the even wave function

$$\Phi_i^S(X) = \begin{cases} 0 & (1+r) \leq X < \infty \\ \Psi_I^{iS}(X) & r < X < 1+r \\ \Psi_{II}^{iS}(X) & -r \leq X \leq r \\ \Psi_I^{iS}(-X) & -(1+r) < X < -r \\ 0 & -\infty < X \leq -(1+r) \end{cases} \quad (33)$$

where $i = 1, 2, 3$,

$$\Psi_I^{iS}(X) = \bar{A}_i^S \cos(\gamma c_i^S \pi X) + \bar{B}_i^S \sin(\gamma c_i^S \pi X) \quad (34)$$

and

$$\Psi_{II}^{iS}(X) = \bar{C}_i^S \cosh\left(\gamma \sqrt{1 - (c_i^S)^2} \pi X\right) \quad (35)$$

To get numerical values of Φ_i^S we need to use Eqs.(45a,45b) to get the expressions for \bar{A}_i^S and \bar{B}_i^S as functions of γ , r , c_i^S , and \bar{C}_i^S . Notice that Φ_i^S is defined up to an undetermined

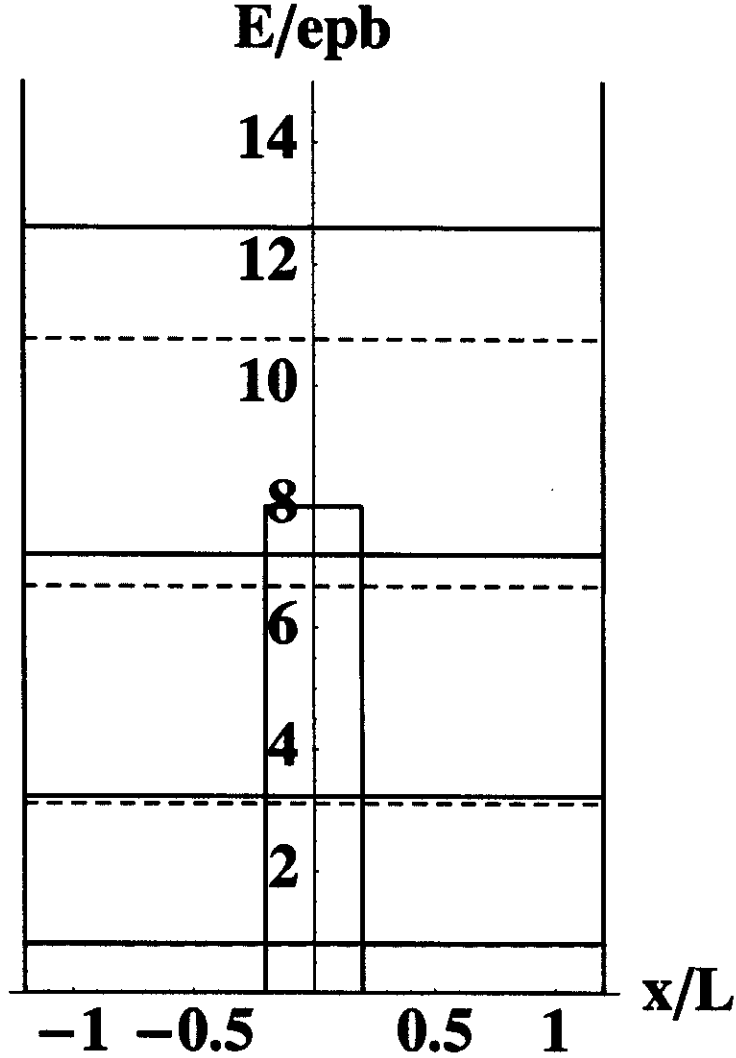


FIG. 5: The first eight energy levels for the double square well box, where we have normalized by measuring energy in units of $epb \equiv \frac{\hbar^2}{8mL^2}$. The dashed lines correspond to even solutions, while the continuous lines correspond to odd solutions.

constant C_i^S that normalizes Φ_i^S e.g.,

$$\int_{-(1+r)}^{1+r} |\Phi_i^S(X)|^2 dX = |\bar{C}_i^S|^2 (N_i^S) = 1 \quad (36)$$

If we define $C_i^S = 1/\sqrt{N_i^S}$, we end up with a normalized wave function, $\Phi_i^S(X)$. In Appendix C we consider similar calculations for the odd solution $\Phi_i^A(X)$.

Our problem is now reduced to numerical integrations to obtain the N_i^S values, which we obtain using MATHEMATICA 5 in a G4 PowerBook with 1GB of RAM memory and

running at 1.33 GHz. All of the integrals considered in this work can be obtained numerically in less than a minute of real time.

TABLE 2	
$E < V_0$	
$N_1^S = 78.49$	$N_1^A = 83.67$
$N_2^S = 11.77$	$N_2^A = 11.08$
$N_3^S = 2.26$	$N_3^A = 0.57$

Using the N_i^S values in Table 2, we can plot in Figure 6 the first three symmetric normalized solutions for $\gamma = \sqrt{8}$, and $r = 0.20$, and, in Figure 7 we use the N_i^A values to plot the first three asymmetric solutions. These solution are plots derived from exact expressions of the solutions of the Schrödinger Equation for the Square Double Well Potential..

Using our accurate expressions of the wave functions, we can analyze to any extent the spatial properties of each solution and the expected values of the operators associated with observables, e.g. $\langle \hat{X} \rangle$, $\langle \hat{X}^2 \rangle$, $\langle \hat{P} \rangle$, and $\langle \hat{P}^2 \rangle$.

VI. QUANTUM TUNNELING

Quantum mechanics predict that even if the system has an energy less than the barrier's height. it has a finite probability to cross or tunnel the barrier to the other side of the potential barrier. Chemical systems characterized by a two minima potential, like ammonia, are good examples of quantum tunneling. In the case of ammonia this phenomenon is characterized by the energy difference between the first two energy levels, which is in the microwave region.

The DSWP also shows a small energy ting and therefore quantum tunneling. To study this quantum effect, we consider the first two wave functions, which are depicted in more detail in Figures 8, refwfa. The symmetric wave function has a lower energy than the asymmetric wave function, and both have a maximum value at $X = (1+r)/2$. So both solutions predict an equal probability to find the particle on either side of the barrier. Notice that if we add these function a cancelation occurs at the left side of the barrier, while at the right-hand side we get constructive interference. In other words, the sum of these functions represents the localization of the particle to the right-side of the barrier. Therefore the following time

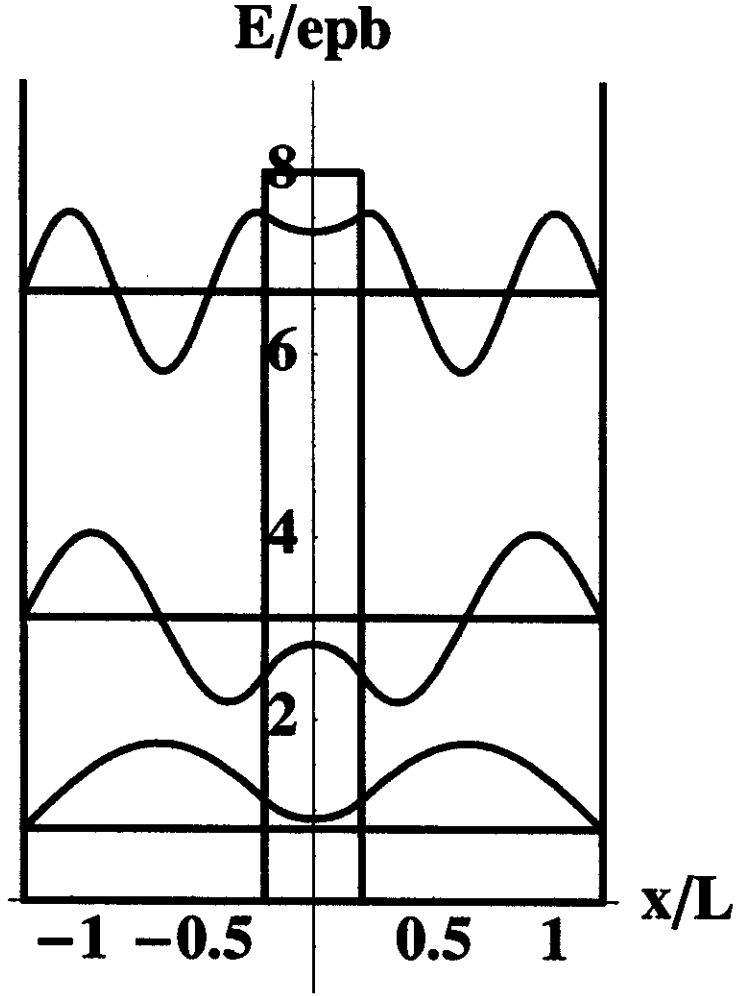


FIG. 6: First three symmetric solutions for $E < V_0$.

dependent wave function is localized to the right side of the barrier at $\tau = 0$:

$$\Phi(X, \tau) = \frac{1}{\sqrt{2}} [\Phi_1^S(X) \exp(-\iota 2\pi E_1^S \tau) + \Phi_1^A(X) \exp(-\iota 2\pi E_1^A \tau)] \quad (37)$$

where we measure distance in units of L , energy in units of epb , and time in units of \tilde{t} defined as

$$\tilde{t} = \frac{8mL^2}{h} \quad (38)$$

To consider quantum tunneling, we calculate the square of the absolute value of $\Phi(X, \tau)$, eq

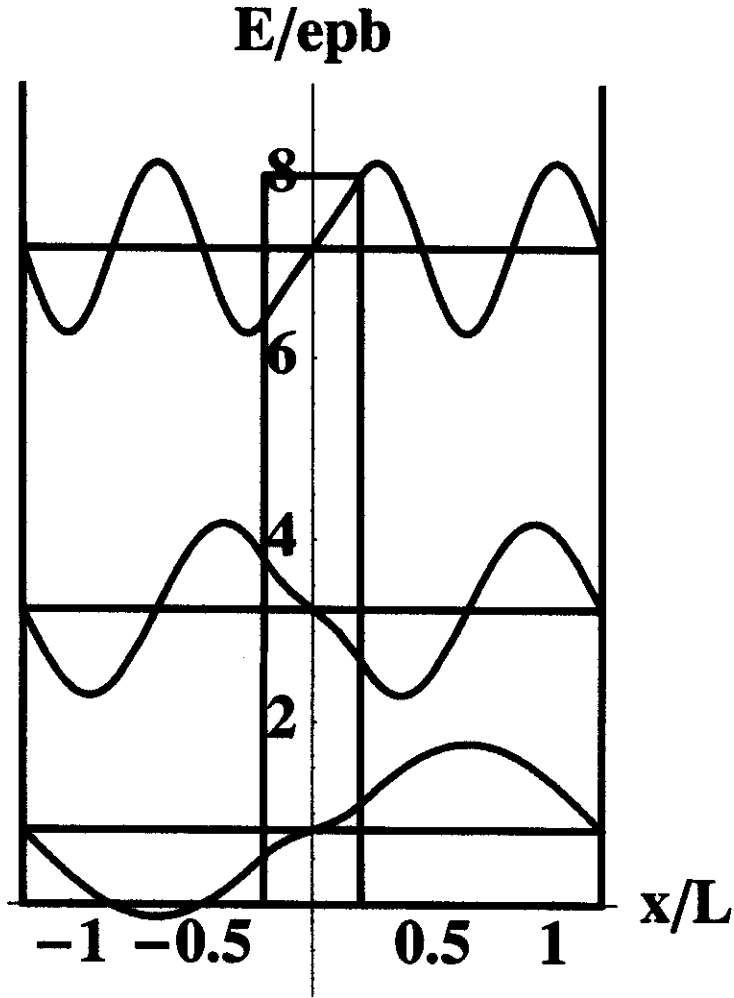


FIG. 7: First three asymmetric solutions for $E < V_0$.

37,

$$P(X, \tau) = \frac{1}{2} [\Phi_1^S(X)^2 + \Phi_1^A(X)^2 + \Phi_1^S(X) \Phi_1^A(X) \cos(2\pi \Delta E_{AS} \tau)] \quad (39)$$

which represents the probability density to find the particle at X and τ . In Figure 10 we plot the initial, $\tau = 0$, probability density, which clearly shows the localization to the right of the barrier. In Figure 11 we plot the probability density for two times. At $\tau = 12.5$ where we see that the particle has the same probability to be either to the right or left of the barrier. Next we consider $\tau = 25.0$, at which time the particle has gone through the barrier even

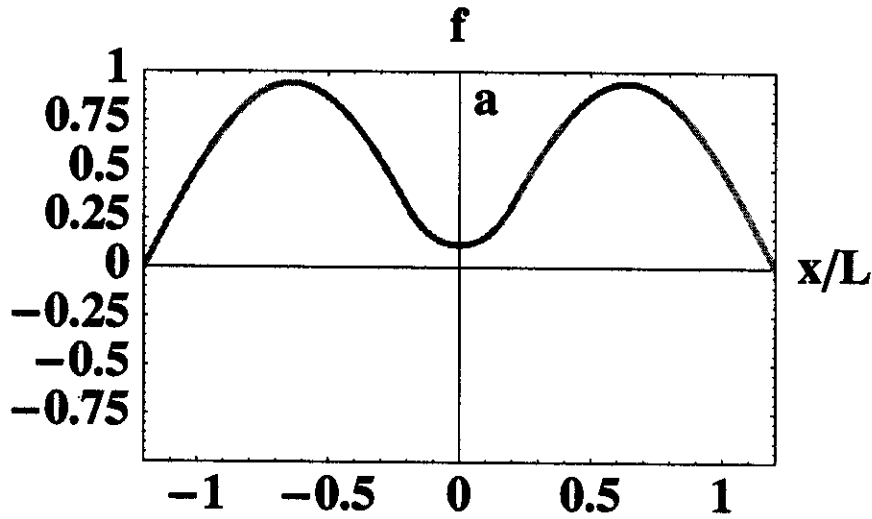


FIG. 8: The ground state solution.

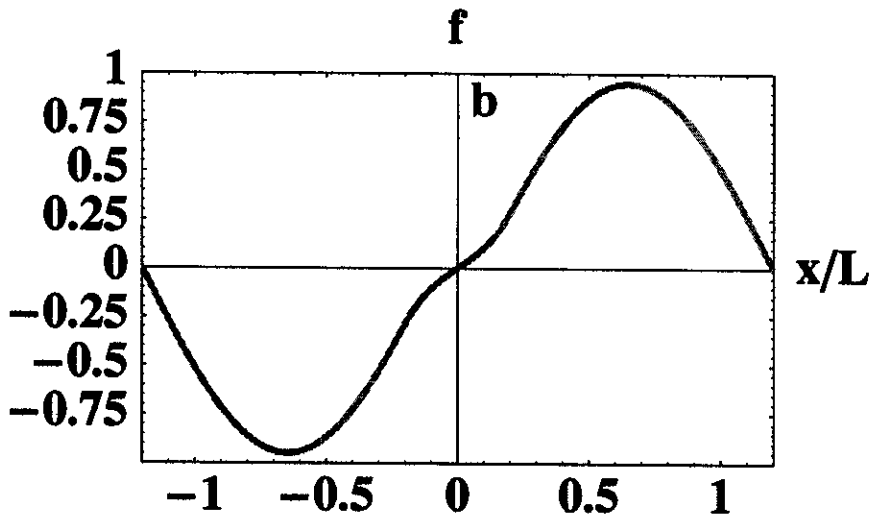


FIG. 9: First asymmetric solution.

though the energies of the first two energy levels are roughly 10% of the barrier's height. Since it takes 25 units of time to move to the left side, the tunneling period is 50 units of time. Finally, we can use our expressions to animate and make a movie of the quantum tunneling process in the DSWP. It is a great video tool in the classroom.

The DSWP clearly shows all the properties of chemical continuous double well potentials considered in the literature. The difference is that in the case of the DWSP we encounter simple straightforward algebraic calculations that yield exact analytical expressions for the

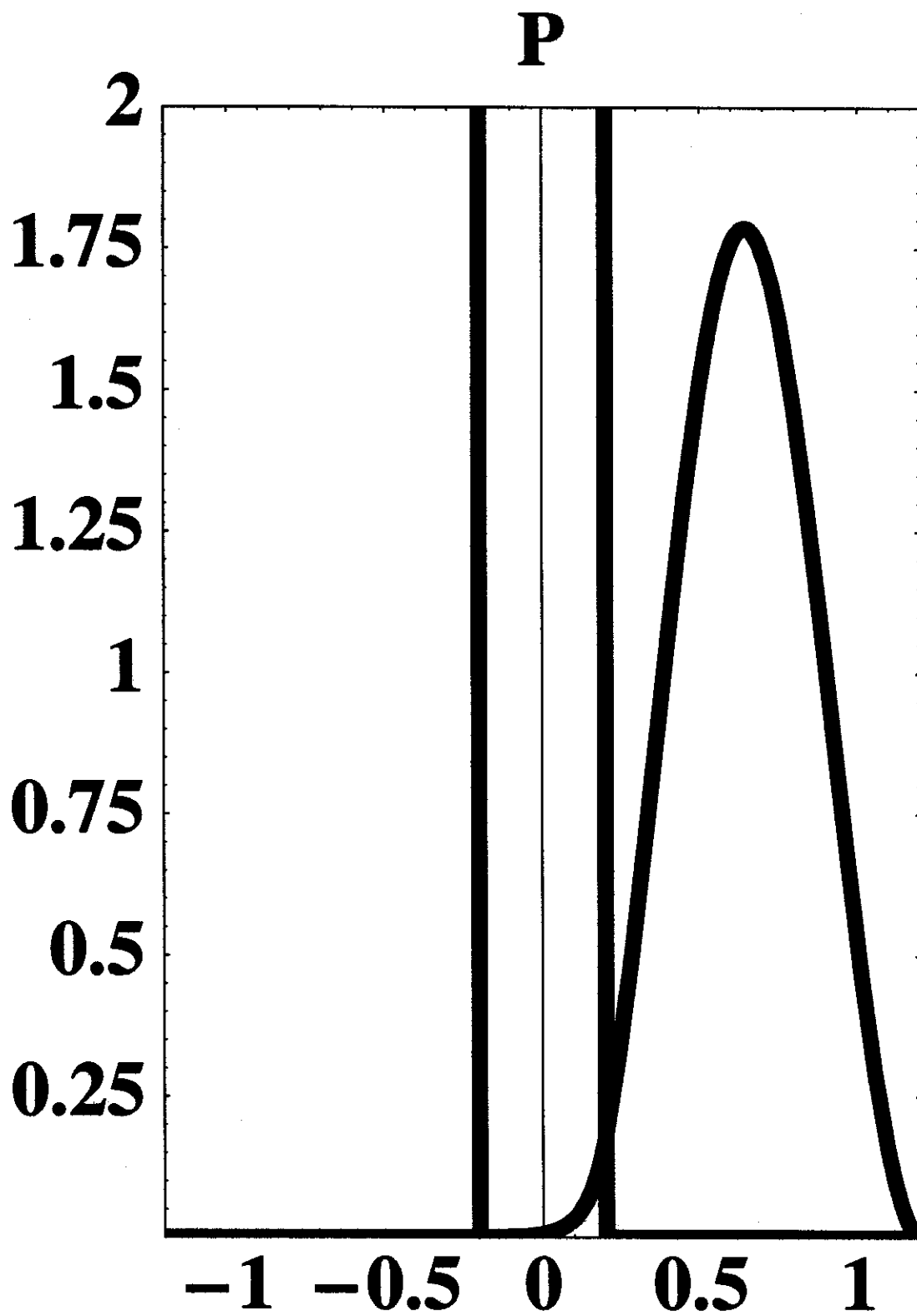


FIG. 10: Initial probability density.

wave functions.

VII. FINAL CALCULATIONS

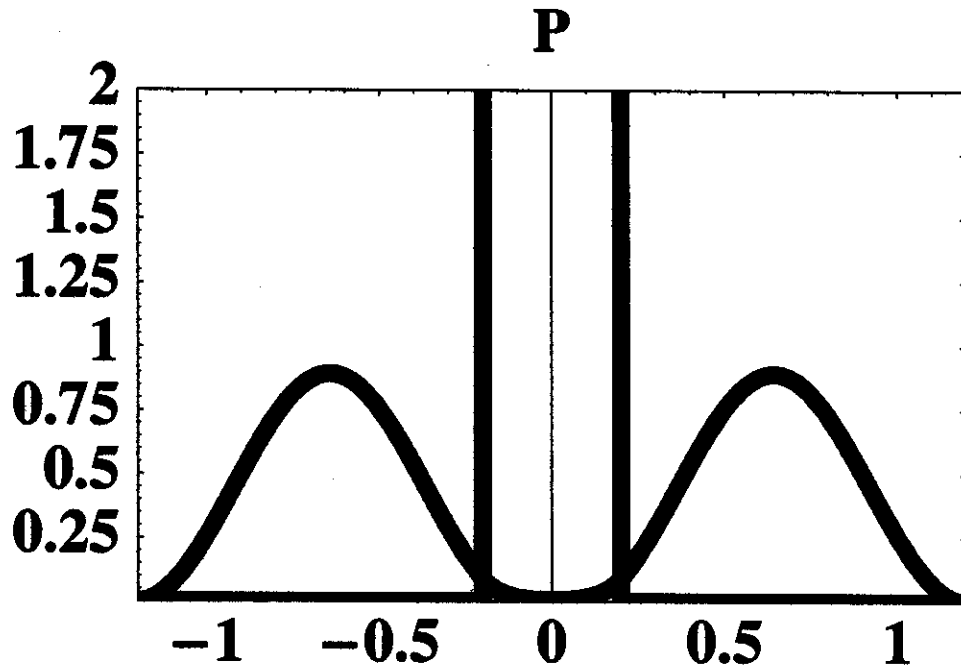
In previous sections we have analyzed, as generally as possible, the solutions of the SE for the DSWP. Now we need to consider a specific chemical system and compare the model with literature data. If we want to model the ammonia molecule with the DSWP, we need to specify the mass, m , and the box length, L . For example we consider the following values in our calculations: $m = 1.00 \times 10^{-26} \text{ kg}$ and $L = 0.50 \times 10^{-10} \text{ m}$. Using these values, we find that our unit of energy, epb, is $1.35 \times 10^{-2} \text{ eV}$ and the unit of time is $0.30 \times 10^{-12} \text{ s}$. With this values we calculate in Table 3 the distance between minima, the barrier's height, the energy difference between the two lowest energy levels, and the tunneling frequency and period. These values are compared with the equivalent experimental values for ammonia.

TABLE 3	
DWSP	Ammonia
$d = 70.0 \text{ pm}$	$d = 75 \text{ pm}$
$V_o = 108 \text{ meV}$	$V_o = 254 \text{ meV}$
$\Delta E_{AS} = 270 \text{ } \mu\text{eV}$	$\Delta E_{SA} = 91.8 \text{ } \mu\text{eV}$
$\nu_T = 6.67 \times 10^{10} \text{ Hz}$	$\nu_T = 2.22 \times 10^{10} \text{ Hz}$
$T = 15 \text{ fs}$	$T = 40 \text{ fs}$

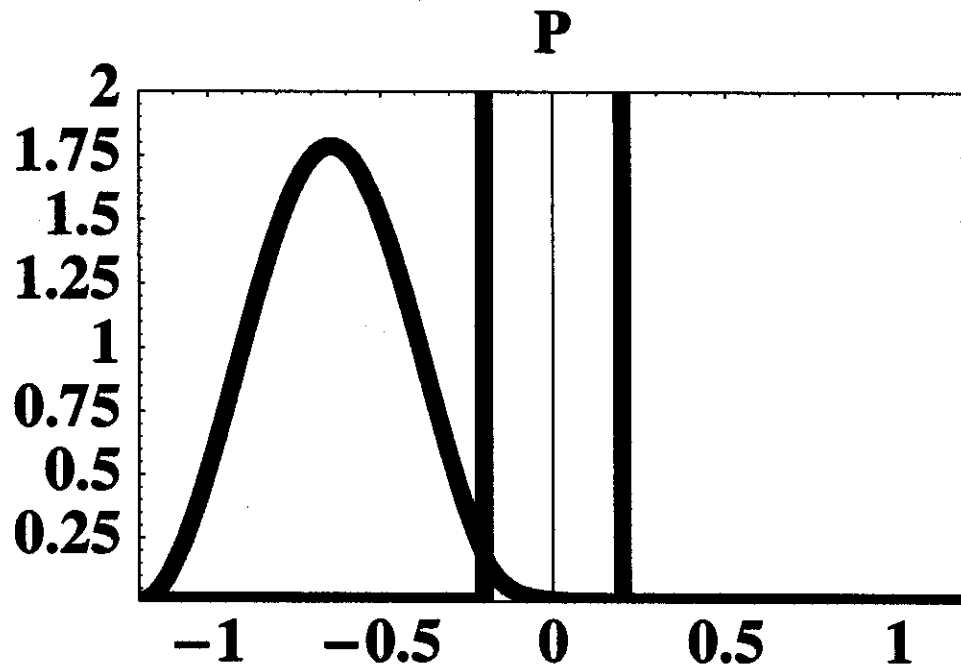
From Table 3 we can see that the DSWP yields values of the same order of magnitude but they are off by a factor of three for the tunneling period and the microwave absorption. Given the gross differences between the DWSP and any experimental continuous double well potential, the calculated values are very good.

VIII. DISCUSSION

In this paper we have studied the DSWP to model double minima potentials. The simplicity of the DSWP allow us to obtain exact relations from the required properties imposed



(a) $P(x, \tau)$ at $\tau = 12.5$.



(b) $P(x, \tau)$ at $\tau = 25$.

FIG. 11: Probability density at a) $\tau = 12.5$ and b) $\tau = 25$, where $|x| < 1.2$.

to the solutions of the Schrödinger equation by the quantum mechanical postulates. The algebraic manipulations are straightforward and accessible to undergraduate students looking for more chemical one-dimensional potential beyond the particle in a box. Although some textbooks briefly include a qualitative discussion of double minima potential, none include an exact quantitative analysis of the DSWP with finite depth, V_D . The numerical aspects of the analysis that include the solution of a transcendental equation and the integration of the solutions of the SE are, nowadays, quite simple with the use of software such as, MATHEMATICA, Maple, MatLab, and MathCad.

The analysis of the DWSP has been used in our advanced course in quantum chemistry, with some of the analysis presented during regular lecture time, where the symmetry properties of the solutions are emphasized. The final numerical analysis is done in one computational lab period, where the progressive ting between the symmetric (even) and asymmetric (odd) solutions is clearly observed. A final animation of the ammonia inversion, as an example of quantum tunneling, is presented in class.

In the case of ammonia, $V_D \approx 20V_o$ [23], which is large enough that our approximation $V_D \gg V_o$ is appropriate. The reader can convince herself that the general case, eq 26a, with $V_D = 20V_o$ shows very small corrections to the values reported here, and the penetration of the wave function for $|x| > L + a/2$ is negligible.

In summary, we discuss a more chemically relevant one-dimensional potential associated with double minima systems and quantum tunneling. The potential goes beyond the traditional and trivial particle in a box analysis, and allow us a quantitative discussion with an animation of the ammonia inversion.

Acknowledgments

The author would like to thank an anonymous referee for reproducing our results using MathCad, Katie Beutel for helpful comments, and the NSF for their financial support through grants CHE-0136143 and CHE-0548622.